Bol. Soc. Paran. Mat.
©SPM – E-ISSN-2175-1188
SPM: www.spm.uem.br/bspm

(3s.) **v. 2025 (43) 4** : 1–11.
ISSN-0037-8712
doi:10.5269/bspm.78522

Magnetohydrodynamic Stokes Flow of Couple Stress Fluid Past a Viscous Liquid Drop in a Porous Medium

Sivaprasad Jammula[1] and Phani Kumar Meduri[2]*

ABSTRACT: This article analyzes the steady flow of couple stress fluid past a viscous liquid droplet embedded in a porous medium under the influence of a magnetic field, employing a no-slip condition. The Stokes and Brinkman equations examine the flow dynamics within and around the liquid drop. The influence of an external magnetic field on fluid flow is characterized by Lorentz's force in the transverse direction. Analytical expressions for stream functions and drag force on a liquid drop are derived. The analysis yields specific cases, such as viscous fluid flow past a viscous liquid drop and a solid sphere, with results in strong agreement with established literature. Graphical analysis illustrates the relationship among the coefficient of drag, couple stress parameter, and Hartmann number. At low couple stress parameter values, strong couple stress effects result in higher drag. The drag also increases with the rising Hartmann number. Streamline patterns are analyzed about different couple stress parameters and Hartmann numbers.

Key Words: magnetohydrodynamic (MHD), couple stress fluid (CSF), drag, liquid drop, no-slip.

Contents

1 Introduction **1**

2 Modelling **3**

3 Solution **5**

4 Drag force **6**

5 Results and discussion **7**

6 Conclusions **9**

1. Introduction

The behavior of non-Newtonian fluids, particularly couple stress fluids, has become a focal point in fluid mechanics due to their ability to model microstructural effects in complex media. The couple stress theory, initially formulated by Stokes, incorporates the effects of particle rotations and characteristic length scales, which are essential in fluids like synovial fluid, blood, and polymer suspensions. Understanding the flow of such fluids past spherical interfaces is vital for biomedical engineering, microfluidics, and material science applications, especially when the sphere is a viscous fluid rather than a solid. Applying an external magnetic field transversely to the flow direction introduces magnetohydrodynamic effects, complicating the flow behavior by introducing Lorentz forces that modify the velocity and stress fields. The combined effects of couple stresses, magnetic forces, porous medium, and interfacial dynamics between the surrounding fluid and the viscous liquid drop constitute a complex and significant issue in practical applications. These configurations occur in practical applications such as magnetically guided drug delivery, industrial filtration, enhanced oil recovery, nanofluid cooling technologies, and electromagnetic control in metallurgical processes, where accurate flow manipulation is essential.
G. G. Stokes [1] laid the theoretical foundation for viscous flow by deriving internal fluid friction equations at low Reynolds numbers. Hartmann [2] initially showed that a uniform magnetic field suppresses laminar flow in electrically conducting fluids by inducing a resistive Lorentz force. Brinkman [3] extended Darcy's law by including viscous shear effects, formulating the Brinkman equation for flow in a porous

* Corresponding author.
2020 *Mathematics Subject Classification:* 7610, 76A05, 76S05.
Submitted August 21, 2025. Published November 01, 2025

medium. This fundamental research facilitates enhanced fluid dynamics modeling inside porous matrices comprised of closely packed particles. Chester [4] initially examined the flow of a viscous, incompressible, electrically conducting fluid around a spherical within a parallel magnetic field. He altered the conventional Stokes drag solution by including a uniform magnetic field at infinity and aligned with the fluid's flow direction. Blerkom Van [5] examined the magnetohydrodynamic flow of a viscous, conductive fluid around a sphere with the aligned flow and magnetic field, emphasizing the force dynamics throughout several regimes. His research provided preliminary insights into the influence of magnetic fields on spherical flow dynamics. Stokes [6] formulated the couple stress fluid theory, introducing couple stress effects to account for rotational motions and microstructural influences in viscous flow. Stokes [7] investigated the effects of couple stresses on creeping flow past a sphere, introducing microstructural fluid behavior into the classical Stokes flow problem. His work highlighted how couple stress fluids deviate from Newtonian predictions, particularly in drag characteristics around spherical bodies. Ramkissoon [8] investigated the influence of couple stresses on fluid flow, revealing their significant role in modifying drag forces on immersed bodies. Happel and Brenner [9] delivered an exhaustive analysis of low Reynolds number hydrodynamics, encompassing both theoretical and practical dimensions of slow viscous flows. Their research provides a fundamental reference for examining creeping flows around particles, such as spheres, in diverse fluid settings. Kyrlidis et al. [10] studied conducting fluid crawling over axisymmetric objects in an aligned magnetic field. They showed that stronger magnetic fields create thin boundary layers and stationary zones near the body. This significantly increases drag, revealing magnetohydrodynamic effects in low Reynolds number flows. Sekhar et al. [11] developed a two-dimensional axisymmetric model to investigate continuous magnetohydrodynamic flow around a sphere in an aligned magnetic field. Their findings demonstrated nonlinear fluctuations in recirculation and a linear escalation in drag corresponding to the interaction parameter. Devakar and Iyengar [12] analyzed Stokes' first and second problems for incompressible couple stress fluids, highlighting the influence of couple stress effects on unsteady viscous flow near boundaries. Devakar et al. [13] investigated analytical solutions for several fully developed flows of Couple Stress fluids that were contained within concentric cylinders with slip boundary conditions. Jaiswal [14] investigated the viscous flow around a Reiner-Rivlin liquid sphere submerged in a saturated porous media, employing the Brinkman equation to analyze the flow within the porous medium. Murthy and Kumar [15] derived an exact solution for Stokes flow over a contaminated fluid sphere by applying a no-slip condition at the fluid interface, offering insights into interfacial effects on low Reynolds number flows. Ashmawy [16] investigated the drag force on a slip spherical particle in a couple stress fluid, demonstrating how couple stress effects and slip conditions modify particle motion and resistance. Madasu and Bucha [17] investigated magnetohydrodynamic flow within a fluid-filled spherical cell by employing Happel's and Kuwabara's boundary conditions to simulate flow and stress continuity. Their methodology encapsulates the interplay between the internal fluid sphere and the external medium influenced by magnetic forces. Siddique and Umbreen [18] provided analytical solutions for incompressible couple stress fluid flows employing Laplace and Fourier transform methods. Their research emphasizes the influence of couple stresses on velocity profiles throughout time and differing Reynolds numbers. Madasu and Bucha [19] investigated magnetohydrodynamic creeping flow around a weakly permeable spherical particle utilizing cell models that integrate Stokes and Darcy flow. They examined the influence of magnetic fields, permeability, and volume fraction on drag and hydrodynamic behavior. Selvi et al. [20] examined creeping flow surrounding a non-Newtonian liquid sphere within a porous medium, employing Brinkman and Stokes models. Their findings underscore the influence of viscosity ratio, permeability, and non-Newtonian characteristics on drag force dynamics. Kunche and Meduri [21] used analytical methods to study micropolar fluid flow across a sphere under interfacial slip. The study also examined stream functions and drag on spheres when micropolar fluids flow past Newtonian fluid spheres and vice versa. Madasu and Sarkar [22] analytically studied the flow of a couple stress fluid past a sphere under a magnetic field, revealing the combined impact of couple stress effects and magnetohydrodynamic forces on flow characteristics. Wang et al. [23] conducted an analytical investigation of the MHD clamshell instability on a sphere characterized by opposing tilts of magnetic field lines over the equator. Their research, driven by solar tachocline dynamics, provides insights into the evolution of instability under mild shear circumstances. Devi and Meduri [24] analyzed the flow of a couple stress fluid around a polluted fluid sphere under slip boundary circumstances. Their research

elucidates the impact of interfacial slip and contamination on flow dynamics and drag forces in intricate fluid systems. Maurya et al. [25] investigated the influence of a magnetic field on the flow of a couple stress fluid surrounding a solid sphere within a porous medium. They found that the drag force diminishes with increased couple stress parameters. Meduri and Kunche [26] analytically calculated the drag force for a viscous fluid flowing past a contaminated micropolar fluid droplet, as well as for a viscous fluid flowing past a contaminated viscous fluid droplet situated in a confined porous medium. Sakthivel and Shukla [27] used the method of separation of variables to determine the stream function and corresponding drag force on a solid spherical particle enclosed in a Newtonian liquid sphere and immersed in a couple stress fluid medium. Alotaibi and El-Sapa [28] illustrated the role of the Lorentz force in liquid density, considering a homogeneous and isotropic medium while neglecting couple stress and body force effects in the flow direction. Meduri et al. [29] presented an exact solution for couple stress fluid flow past a fluid sphere in a porous medium with slip, highlighting the effects of couple stresses, porosity, and slip-on flow behavior. Ramasamy and Chauhan [30] investigated the creeping flow of a couple stress fluid past a semipermeable spherical particle with a solid core, examining the combined influence of couple stress effects and an external magnetic field. Jammula and Meduri [31] derived an exact solution for laminar viscous flow over a contaminated liquid drop in a porous medium, emphasizing the effects of surface contamination and magnetohydrodynamics on flow behavior.

This work examines the flow of couple stress fluid past a viscous liquid drop placed in a porous medium under magnetic effect. It aims to derive an analytical solution for stream functions and compute the drag force acting on the liquid drop and the coefficient of drag employing no-slip boundary conditions. Couple stress fluid flow past a viscous liquid drop study applies to magnetic drug delivery, microfluidics, and adaptive suspension systems, such as using magnetorheological fluids in vehicle suspension for smoother rides.

2. Modelling

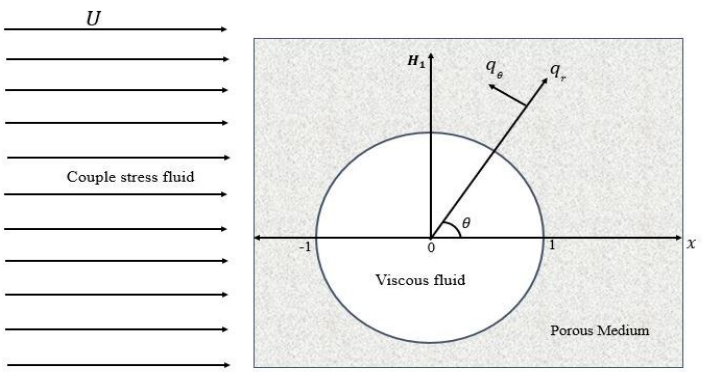

Figure 1: Geometry of proposed model

Consider the axisymmetric, steady, incompressible CSF flow past a liquid drop of radius 1 under the applied uniform magnetic field $\widetilde{H_1}$, which is considered in the transverse direction of the flow with uniform fluid velocity U, as shown in Figure1. Also, in the absence of an external electric field and for a very small magnetic Reynolds number, we can neglect the induced electric current. Here, the induced magnetic field is taken to be very small in comparison to the external magnetic field. In addition, the permeability k of the porous medium is considered.

Lorentz force is $\widetilde{F} = \widetilde{J} \times \widetilde{H_1}$ i.e., $F = \mu_h^2 \, \sigma_e \left(\widetilde{q} \times \widetilde{H_1}\right) \times \widetilde{H_1}$, where $\widetilde{H_1}$ is magnetic induction vector, $\widetilde{J}$ is the electric current density, σ_e is the electric conductivity of the fluid and μ_h is the magnetic permeability of the fluid.

Consider $(r, \ \theta, \ \emptyset)$ as the spherical co-ordinate system.

The current flow is slow, axially symmetric and stable, resulting in independent physical parameters

associated with it $\emptyset$.
Thus, velocity vector of the internal and external regions is given by
$\widetilde{q} = \ q_r\,(r,\theta)\ \widetilde{e}_r + q_\theta\,(r,\theta)\,\widetilde{e}_\theta$.
Expressing velocity components in terms of stream function Ψ which satisfy the continuity equation as

$$q_r = -\frac{1}{\widetilde{r}^2\ sin\theta}\frac{\partial \Psi}{\partial \theta}, \quad q_\theta = \frac{1}{\widetilde{r}\ sin\theta}\frac{\partial \Psi}{\partial \widetilde{r}}. \tag{2.1}$$

Consider $\Psi \ = \ \Psi_i$ for the internal region and $\Psi \ = \ \Psi_e$ for the external region.
The governing equations for the steady flow of an incompressible viscous fluid in the internal region of liquid drop by Stokes [1] equation are given by

$$\widetilde{\nabla}\ .\ \widetilde{q_i} = 0, \tag{2.2}$$

$$\widetilde{\nabla} p_i + \mu_i \widetilde{\nabla}\ \times\ \widetilde{\nabla}\ \times \widetilde{q_i} = 0. \tag{2.3}$$

The governing equations for the steady flow of an incompressible couple stress fluid in the external region of liquid drop by Brinkman's [3] conditions are given by

$$\widetilde{\nabla}\ .\ \widetilde{q_e} = 0, \tag{2.4}$$

$$\widetilde{\nabla} p_e + \ \mu_e\ \widetilde{\nabla}\ \times\ \widetilde{\nabla}\ \times\ \widetilde{q_e} + \eta_e \widetilde{\nabla}\ \times\ \widetilde{\nabla}\ \times \widetilde{\nabla}\ \times \widetilde{\nabla}\ \times \widetilde{q_e} + \ \frac{\mu_e}{k}\widetilde{q_e} - \mu_h^2\ \sigma_e\ \left(\widetilde{q_e}\ \times\ \widetilde{H_1}\ \right)\ \times\ \widetilde{H_1}\ \ = 0, \tag{2.5}$$

where $\widetilde{q_i}$ is the internal fluid velocity, $\widetilde{q_e}$ is the external fluid velocity, p_i is the internal fluid pressure, p_e is the external fluid pressure, μ_i is coefficient of viscosity in the internal fluid, μ_e is coefficient of viscosity in the external fluid, η_e is couple stress viscosity coefficient in the external fluid, k is the porous medium permeability, $a = 1$ is the radius of the sphere, σ_e is the electric conductivity of the fluid, μ_h is the magnetic permeability of the fluid.
"The non-dimensional parameters are
$\widetilde{r} = a\ r,\ \widetilde{q_i} = \ U\ q_i,\ \widetilde{q_e} = U\ q_e, \widetilde{H_1} = H_0\ H_1, \Psi = U\ a^2\ \psi,\ \widetilde{\nabla}\ = \frac{\nabla}{a}$." (Meduri et al. [29]).
Substituting above terms in Equations (2.2) - (2.5), we get

$$\nabla\ .\ q_i = 0, \tag{2.6}$$

$$\nabla p_i + \ \nabla\ \times\ \nabla\ \times\ q_i = 0, \tag{2.7}$$

$$\nabla\ .\ q_e = 0, \tag{2.8}$$

$$\nabla p_e + \ \nabla\ \times\ \nabla\ \times\ q_e + \frac{1}{\lambda_e^2}\nabla\ \times\ \nabla\ \times \nabla\ \times \nabla\ \times\ q_e + \ \sigma^2\ q_e - \ \ H^2\ (q_e\ \times\ H_1)\ \times\ H_1 = 0, \tag{2.9}$$

where $\lambda_e^2\ =\ \frac{a^2\mu_e}{\eta_e}, \sigma^2\ =\ \frac{a^2}{k}, H = \sqrt{\frac{\mu_h^2\ H_0^2\ a^2\ \sigma_e}{\mu_e}}$ is the Hartmann number, σ is the porosity parameter, and λ_e is the couple stress parameter of fluid in the external region of liquid drop.
By using non-dimensional scheme and by eliminating the pressure terms from the Equations (2.7) and (2.9), we get momentum equations as

$$E^4 \psi_i = 0, \tag{2.10}$$

$$E^2\left(E^2\ -\ \sigma_2^2\right)\left(E^2\ -\ \sigma_3^2\right)\psi_e = 0, \tag{2.11}$$

where $\sigma_2^2+\sigma_3^2 = \lambda_e^2, \sigma_2^2\ \sigma_3^2 = \lambda_e^2\ \sigma_1^2$, where $\sigma_1^2 = \sigma^2+H^2$ and $E^2 \equiv \frac{\partial^2}{\partial r^2}+\frac{1}{r^2}\frac{\partial^2}{\partial\theta^2}-\frac{cot\theta}{r^2}\frac{\partial}{\partial\theta}$.
The general solutions of the Equations (2.10) and (2.11) can be obtained by using separation of variables as

$$\psi_i = \left[a_5 r^2 + a_6\ r^4 + a_7 r + \ a_8\left(\frac{1}{r}\right)\right]\frac{1}{2}sin^2\theta, \tag{2.12}$$

and

$$\psi_e = \left[a_1\ r^2 + a_2\left(\frac{1}{r}\right) + a_3\sqrt{r}\ K_{\frac{3}{2}}(\sigma_2\ r) + a_4\sqrt{r}K_{\frac{3}{2}}(\sigma_3\ r)\right]\frac{1}{2}sin^2\theta, \tag{2.13}$$

where $K_{\frac{3}{2}}(*)$ are modified Bessel functions of second kind of order $\frac{3}{2}$.
Coefficients are obtained by using the following boundary conditions.

1. Regularity conditions:

   a) Far away from the liquid drop, the flow is uniform, i.e.,

   $$\lim_{r\to\infty}\psi_e = \frac{1}{2}r^2 sin^2\theta. \tag{2.14}$$

   b) Velocity at the origin is finite, i.e.,

   $$\lim_{r\to 0}\psi_i = \text{finite}. \tag{2.15}$$

2. Impermeability condition: On the boundary normal velocity is zero, i.e.,

   $$\psi_i = \psi_e = \ 0 \text{ on } r \ = \ 1. \tag{2.16}$$

3. No-slip condition: Tangential velocity is continuous across the surface, i.e.,

   $$\frac{\partial\psi_e}{\partial r} \ = \frac{\partial\psi_i}{\partial r} \text{ on } r \ = \ 1. \tag{2.17}$$

4. The liquid drop's contact experiences continual shear stress, i.e

   $$\tau_{r\theta e} = \tau_{r\theta i}, \text{ where } \tau_{r\theta} \ = \ \mu_e\left(\frac{1}{r}\frac{\partial q_r}{\partial\theta}+\frac{\partial q_\theta}{\partial r}-\frac{q_\theta}{r}\right)-\frac{1}{2}\left(\frac{1}{r}\frac{\partial M_{\theta\emptyset}}{\partial\theta}+\frac{\partial M_{r\emptyset}}{\partial r}+\frac{2M_{r\emptyset}+M_{\emptyset r}}{r}\right). \tag{2.18}$$

5. Type A condition: Couple stress disappears at the boundary, i.e.,

   $$M_{r\phi} = 0 \text{ on } r = 1. \tag{2.19}$$

3. Solution

By using regularity conditions (2.14) and (2.15), we get $a_1 \ = \ 1,\ a_7 \ = \ 0$, and $a_8 \ = \ 0$. By applying the remaining boundary conditions (2.16) – (2.19), we get system of equations as

$$\left.\begin{array}{l} a_2 + a_3\ K_{\frac{3}{2}}(\sigma_2) + a_4\ K_{\frac{3}{2}}(\sigma_3) = \ -1, \\ a_5 + \ a_6 = \ 0, \\ a_2 + a_3\ K_{\frac{3}{2}}(\sigma_2)\,\Delta_1(\sigma_2) + a_4\ K_{\frac{3}{2}}(\sigma_3)\,\Delta_1(\sigma_3) + 2a_5 + 4a_6 = 2, \\ 6\ a_2 + \left[4+2\Delta_1(\sigma_2)+\sigma_1^2\right]a_3\ K_{\frac{3}{2}}(\sigma_2) + \left[4+2\Delta_1(\sigma_3)+\sigma_1^2\right]a_4\ K_{\frac{3}{2}}(\sigma_3) - 6\ \mu\ a_6 = 0, \\ \sigma_2^2\left[\Delta_1(\sigma_2)+1+e\right]a_3\ K_{\frac{3}{2}}(\sigma_2) + \sigma_3^2\left[\Delta_1(\sigma_3)+1+e\right]a_4\ K_{\frac{3}{2}}(\sigma_3) = 0, \end{array}\right\} \tag{3.1}$$

where $e = \frac{\eta'}{\eta}$ is couple stress viscosity ratio (CSVR).
By solving these equations, we get

$$\left.\begin{aligned} a_2 &= \frac{3\left[M_2\Delta_1(\sigma_2) - M_1\Delta_1(\sigma_3) + 2M_2 - 2M_1\right]\mu + \left[M_2M_3 - M_1M_4\right]}{M} \\ a_3 &= -\frac{3M_2\left[3\mu+2\right]}{M\ K_{\frac{3}{2}}(\sigma_2)}, \\ a_4 &= \frac{3M_1\left[3\mu+2\right]}{M\ K_{\frac{3}{2}}(\sigma_3)}, \\ a_5 &= -\frac{3\ \sigma_1^2\ \left[M_1 - M_2\right]}{2\ M} \\ a_6 &= \frac{3\ \sigma_1^2\ \left[M_1 - M_2\right]}{2\ M}, \end{aligned}\right\} \tag{3.2}$$

The all values of M's are given in Appendix.
Consequently, all coefficients are determined and substituted into equations (2.12) and (2.13) to obtain the stream function expressions for the internal and external regions.

4. Drag force

The drag force (F_z) on the liquid drop is evaluated using the formula Happel and Brenner [9],

$$F_z = 2\ \pi\ a^2\ \left\{\int_0^{\pi}\ \left(\tau_{rr}\ cos\theta - \ \tau_{r\theta}\ sin\theta\right)_{r\ =\ 1}\ \ sin\theta\ d\theta\right\}, \tag{4.1}$$

where $\tau_{rr}\ = -\ p\ +\ 2\ \mu_e \frac{\partial q_r}{\partial r}$.
By substituting the values of τ_{rr} and $\tau_{r\theta}$ and simplifying, we get F_z as

$$F_z = -\frac{2}{3}\pi\mu_e U\sigma_1^2\left(-2 + \ a_2 - 2\ a_3\ \ K_{\frac{3}{2}}(\sigma_2) - 2\ a_4\ \ K_{\frac{3}{2}}(\sigma_3)\right), \tag{4.2}$$

Substituting values from Equation (3.2), we get

$$F_z = 2\pi U\mu_e\sigma_1^2\left[\frac{3\left[M_1\Delta_1(\sigma_3) - M_2\Delta_1(\sigma_2) + 2M_1 - 2M_2\right]\mu + \left[M_1M_4 - M_2M_3\right]}{M}\right], \tag{4.3}$$

and coefficient of drag (C_D) = $\frac{F_z}{\frac{1}{2}\ \rho\ \pi\ U^2}$.

$$C_D = \frac{8}{Re}\sigma_1^2\ \left[\frac{3\left[M_1\Delta_1(\sigma_3) - M_2\Delta_1(\sigma_2) + 2M_1 - 2M_2\right]\mu + \left[M_1M_4 - M_2M_3\right]}{M}\right], \tag{4.4}$$

where $Re = \frac{2\rho U}{\mu_e}$.

Special cases:

1. If $H = 0$ and $\sigma = 0$, we get couple stress fluid flow past a viscous liquid drop with no magnetic effect and no porous medium. Then

   $F_z = 6\pi U\mu_e\left[\frac{\lambda_e^2[\Delta_1(\lambda_e)+1+e][3\mu+2]}{\lambda_e^2[\Delta_1(\lambda_e)+1+e][3\mu+3]-[\Delta_1(\lambda_e)-1][3\mu+2][1+e]}\right]$, and

   $C_D = \frac{24}{Re}\left[\frac{\lambda_e^2[\Delta_1(\lambda_e)+1+e][3\mu+2]}{\lambda_e^2[\Delta_1(\lambda_e)+1+e][3\mu+3]-[\Delta_1(\lambda_e)-1][3\mu+2][1+e]}\right]$,

   which agrees with the result of Sakthivel and Shukla [27].

2. If $H = 0$, $\sigma = 0$ and $\lambda_e \to \infty$, this becomes as a viscous fluid flow past a viscous liquid drop with no magnetic effect and no porous medium. Then

   $F_z = 6\pi\ U\ \mu_e \left[\frac{\mu + \frac{2}{3}}{\mu + 1}\right]$, and $C_D = \frac{24}{Re}\left[\frac{\mu + \frac{2}{3}}{\mu + 1}\right]$,

   which agree with the result reported in the book by Happel and Brenner [9] for the drag force experienced by a liquid drop in a fluid medium.

3. If $H = 0, \sigma = 0, \lambda_e \to \infty$, and $\mu \to \infty$, we get viscous fluid flow past a solid sphere with no magnetic effect. Then

   $F_z = 6\ \pi\ U\ \mu_e$ and $C_D = \frac{24}{Re}$,

   which is the well-known Stokes [1] result and reported in the book by Happel and Brenner [9] for flow past a solid sphere in an unbounded medium.

   Thus, the expressions obtained in Equations (4.3) and (4.4) are validated with previous results in the literature.

5. Results and discussion

The effect of altering the couple stress parameter and Hartmann number on the coefficient of drag at fixed dependent parameters is investigated and reported in graphical and tabular formats.

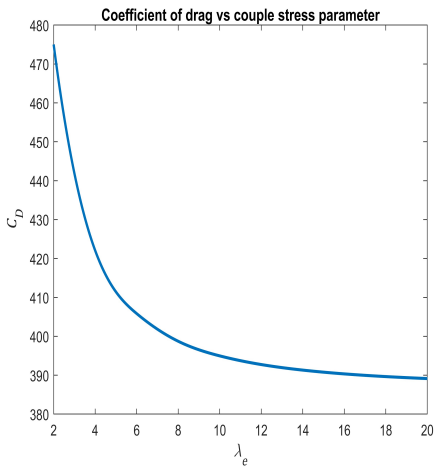

Figure 2: Coefficient of drag (C_D) with couple stress parameter (λ_e) for $H = 1, \sigma = 0.1, \mu = 0.5, e = 0.8$, and $Re = 0.1$.

λ_e	2	4	6	8	10	12	14	16	18	20
C_D	475.03	422.06	405.84	398.73	394.97	392.74	391.31	390.34	389.65	389.14

Table 1: Values of coefficient of drag (C_D) with couple stress parameter (λ_e) for $H = 1, \sigma = 0.1, \mu = 0.5, e = 0.8$, and $Re = 0.1$.

Figure 2 shows the change in the coefficient of drag (C_D) with couple stress parameter (λ_e) for fixed Hartmann number, porosity parameter, viscosity ratio, and couple stress viscosity ratio values. With increasing values of the couple stress parameter, a significant reduction in the drag coefficient is observed, corresponding to a weakening of couple stress effects. At low couple stress parameter values, strong couple stress effects result in higher drag, indicating more resistance to motion due to the increasing influence of couple stress effects. The numerical values are presented in Table 1.

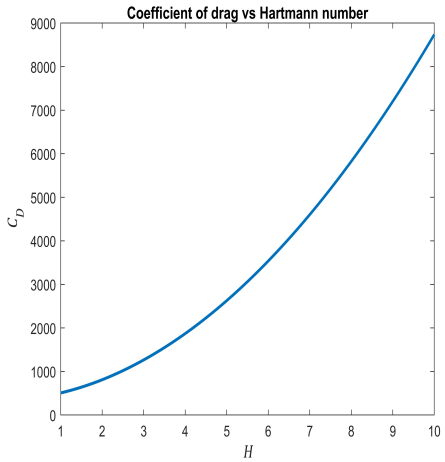

Figure 3: Coefficient of drag (C_D) with Hartmann number (H) for $\sigma = 1,\ e = 0.8, \mu = 0.5, \lambda_e = 15$, and $Re = 0.1$.

H	1	2	3	4	5	6	7	8	9	10
C_D	508.00	810.74	1265.70	1870.50	2627.10	3537.20	4602.30	5823.60	7201.80	8737.50

Table 2: Values of coefficient of drag (C_D) with Hartmann number (H) for $\sigma = 1,\ e = 0.8, \mu = 0.5, \lambda_e = 15$, and $Re = 0.1$.

Figure 3 shows the change in the coefficient of drag (C_D) with the Hartmann number (H) for the fixed viscosity ratio, couple stress parameters, and CSVR values. The coefficient of drag increases with an increase in the Hartmann number, indicating that the flow executes higher resistance to the motion of the liquid drop due to the influence of the magnetic effect. A higher Hartmann number value represents a greater magnetic effect and increases the resistance to motion. The numerical values are presented in Table 2.

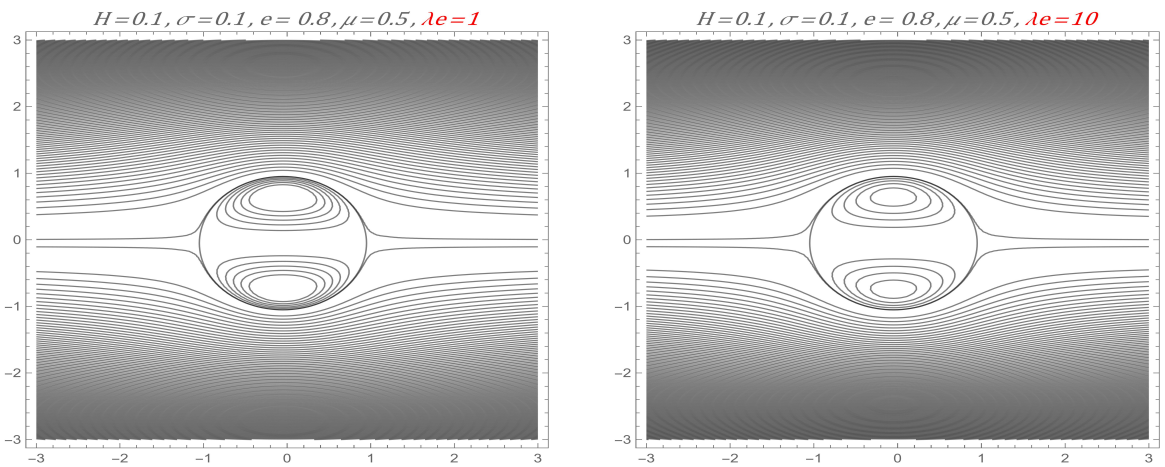

(a) (b)

Figure 4: Streamline plots for different couple stress parameters (a) $\lambda_e = 1$, and (b) $\lambda_e = 10$ at fixed $H = 0.1, \sigma = 0.1,\ e = 0.8,\ \mu = 0.5$.

In Figure 4, for $\lambda_e = 1$, the external streamlines are highly curved and densely packed near the viscous sphere, indicating strong couple stress effects and significant flow disturbance. As λ_e increases to 10, the streamlines become smoother and more parallel, reflecting a shift toward Newtonian-like external flow. Internally, the viscous fluid shows tighter closed streamline loops due to higher shear interaction at low λ_e. With increasing λ_e, the interface shear weakens, resulting in more relaxed internal streamlines and less distortion in the external flow.

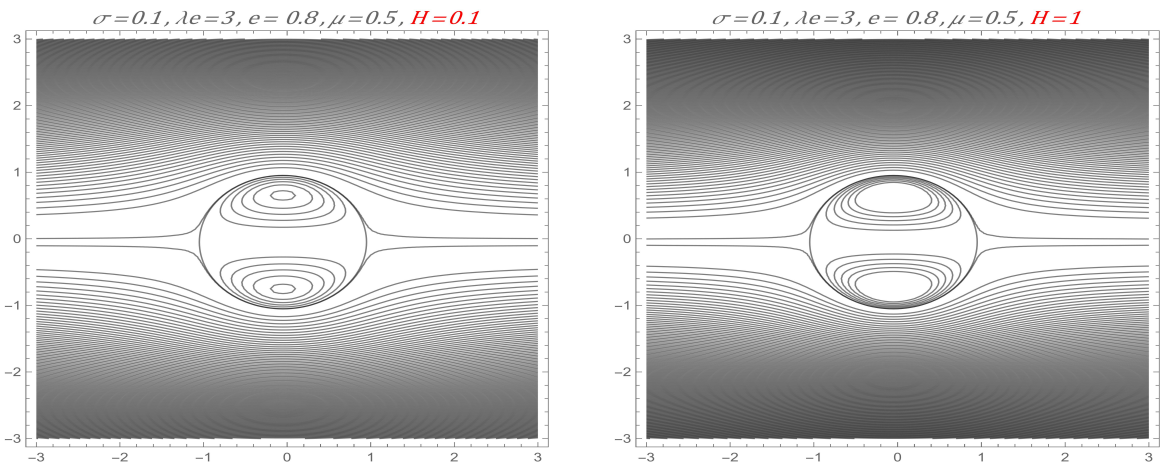

(a) (b)

Figure 5: Streamline plots for different Hartmann numbers (a) $H = 0.1$, and (b) $H = 1$ at fixed $\sigma = 0.1, \lambda_e = 3, e = 0.8, \mu = 0.5$.

In Figure 5, At low Hartmann number $H = 0.1$, the external streamlines are more distorted and curved around the sphere, indicating weaker Lorentz force resistance to flow. As H increases to 1, the streamlines become more parallel and less deviated, showing suppression of transverse motion due to stronger magnetic damping. Internally, denser and more closed streamlines appear at lower H, reflecting stronger induced circulation.

6. Conclusions

We presented an analytical solution for magnetohydrodynamic CSF flow past a viscous liquid drop, utilizing no-slip condition. Analytical expressions for stream functions and drag force on a viscous liquid drop are derived. Specific cases, such as viscous fluid flow past a viscous liquid drop and a solid sphere, are deducted. The effects of the couple stress parameter and Hartmann number on drag are investigated through graphical analysis and tabulated numerical results, while streamlines are employed to visualize the flow characteristics.
We observed the following illustrations in our work:

1. A higher Hartmann number value represents a greater magnetic effect, which increases the resistance to motion, resulting in higher drag.

2. Significant couple stress effects result in heightened drag at low values for the couple stress parameter.

3. As couple stress parameter increases, external streamlines smoothen while internal circulation weakens due to reduced shear transmission.

4. As Hartmann number increases, magnetic damping makes internal streamlines more compact while external streamlines compress vertically.

Future studies may examine other non-Newtonian flows, like micropolar fluid, power law fluid etc., past other non-Newtonian flows influenced by magnetic effects.

References

1. G. G. Stokes, *On the theory of the internal friction in fluids in motion*, Trans. Camb. Phil. SOC., 8, 287–319, (1845).
2. J. Hartmann, *Theory of the laminar flow of an electrically conductive liquid in a homogeneous magnetic field*, Fys. Med., 15, 1 – 27, (1937).
3. H.C. Brinkman, *A calculation of the viscous force exerted by a flowing fluid on a dense swarm of particles*, Appl. Sci. Res., 1, 27-34, (1949).
4. W. Chester, *The effect of a magnetic field on stokes flow in a conducting fluid*, J. Fluid Mech., 3(3), 304–308, (1957).
5. R. Blerkom Van, *Magnetohydrodynamic flow of a viscous fluid past a sphere*, J. Fluid. Mech., 8(3), 432-441, (1960).
6. V. K. Stokes, *Couple Stresses in Fluids*, Physics of Fluids, 9(9), 1709 – 1715, (1966).
7. V.K. Stokes, *Effects of couple stresses in fluids on the creeping flow past a sphere*, Physics of fluids, 14(7), 1580 – 1582, (1971).
8. H. Ramkissoon, *The effect of a magnetic field on stokes flow in a conducting fluid*, J. Fluid Mech., 3(3), 304–308, (1957).
9. J. Happel, and H. Brenner, *Low Reynolds number hydrodynamics*, Martinus Nijoff Publishers, The Hague, (1983).
10. A. Kyrlidis, R.A. Brown, and J.S. Walker, *Creeping flow of a conducting fluid past axisymmetric bodies in the presence of an aligned magnetic field*, Physics of Fluids A: Fluid Dynamics, 2(12), 2230 – 2239, (1990).
11. T.V.S. Sekhar, R. Sivakumar, and T.R. Kumar, *Magnetohydrodynamic flow around a sphere*, Fluid dynamics research, 37(5), 357-373, (2005).
12. M. Devakar, and T.K.V.K.V. Iyengar, *Stokes' problems for an incompressible couple stress fluid*, Nonlinear Analysis: Modelling and Control, 13(2), 181 – 190, (2008).
13. M. Devakar, D. Sreenivasu, and B. Shankar, *Analytical solutions of couple stress fluid flows with slip boundary conditions*, Alexandria Eng. J., 53(3), 723 – 730, (2014).
14. B.R. Jaiswal, and B.R. Gupta, *Brinkman flow of a viscous fluid past a Reiner–Rivlin liquid sphere immersed in a saturated porous medium*, Transport in Porous Media, 107(3), 907-925, (2015).
15. J.R. Murthy, and M.P. Kumar, *Exact solution for flow over a contaminated fluid sphere for Stokes flow*, In Journal of Physics: Conference Series, IOP Publishing, 662(1), 012016, (2015).
16. E.A. Ashmawy, *Drag on a slip spherical particle moving in a couple stress fluid*, Alexandria Engineering Journal, 55(2), 1159 – 1164, (2016).
17. K.P. Madasu, and T. Bucha, *Creeping flow of fluid sphere contained in a spherical envelope: magnetic effect*, SN Applied Science, 1, 1-8, (2019).
18. I. Siddique, and Y. Umbreen, *Analytical solutions of incompressible couple stress fluid flows*, Appl. Math., 13(6), 1009 – 1014, (2019).
19. K.P. Madasu, and T. Bucha, *Magnetohydrodynamic creeping flow around a weakly permeable spherical particle in cell models*, Pramana – Journal of Physics, 94(1), 1–10, (2020).
20. R. Selvi, P. Shukla, and A.N. Filippov, *Flow around a liquid sphere filled with a non-Newtonian liquid and placed into a porous medium*, Colloid Journal, 82, 152-160, (2020).
21. V.L. Kunche, and P.K. Meduri, *Stokes flow of Micropolar fluid beyond fluid sphere with slip condition*, ZAMM-Journal of Applied Mathematics and Mechanics, 102(11), e202100340, (2022).
22. K.P. Madasu, and P. Sarkar, *An analytical study of couple stress fluid through a sphere with an influence of the magnetic field*, Journal of Applied Mathematics and Computational Mechanics, 21(3), 99 – 110, (2022).
23. C.Wang, A.D. Gilbert, and J. Mason, *An analytical study of the MHD clamshell instability on a sphere*, Journal of Fluid Mech., 953, A38, (2022).
24. P.N.L. Devi, and P.K. Meduri, *Couple stress fluid past a contaminated fluid sphere with slip condition*, Applied Mathematics and Computation, 446, 127845, (2023).
25. PK. Maurya, S. Deo, and DK. Maurya, *Couple stress fluid flow enclosing a solid sphere in a porous medium: effect of magnetic field*, Phys. Fluids, 35(7), 072006, (2023).
26. P.K. Meduri, and V.L. Kunche, *Creeping flow about a tainted liquid drop with a micropolar fluid and aligned in a porous medium filled with viscous fluid utilizing slip*, Special Topics and Reviews in Porous Media: An International Journal, 15(6), 61-76, (2024).
27. S. Sakthivel, and P. Shukla, *Motion through a viscous liquid sphere enclosed by a solid core embedded into a Brinkman medium*, ZAMM-Journal of Applied Mathematics and Mechanics, 103(10), e202200601, (2023).

28. M.A. Alotaibi, and S. El-Sapa, *MHD couple stress fluid between two concentric spheres with slip regime*, Results in Engineering, 21, 101934, (2024).

29. P.K. Meduri, N.L.D. Parasa, and V. Lakshmi Kunche, *Exact solution for couple stress fluid flow past a fluid sphere embedded in a porous medium with slip condition*, Journal of Naval Architecture and Marine Engineering, 21(1), 41 – 50, (2024).

30. S. Ramasamy, and S.S. Chauhan, *Creeping flow of a couple stress fluid past a semipermeable spherical particle consisting of a solid core: magnetic field effect*, Journal of the Brazilian Society of Mechanical Sciences and Engineering, 46(8), 489, (2024).

31. S. Jammula, and P.K. Meduri, *Exact solution for laminar viscous fluid flow over a contaminated liquid drop placed in a porous region: magnetohydrodynamics*, Physics of Fluids, 37(1), 013626, (2025).

Appendix:

$$
\begin{aligned}
M_1 &= \sigma_2^2\left[\Delta_1(\sigma_2)+1+e\right],\\
M_2 &= \sigma_3^2\left[\Delta_1(\sigma_3)+1+e\right],\\
M_3 &= 4+2\Delta_1(\sigma_2)+\sigma_1^2,\\
M_4 &= 4+2\Delta_1(\sigma_3)+\sigma_1^2,\\
M &= 3\left[M_1\Delta_1(\sigma_3)-M_2\Delta_1(\sigma_2)+M_2-M_1\right]\mu+\left[M_1M_4-M_2M_3-6M_1+6M_2\right].
\end{aligned}
$$

[1,2] *Department of Mathematics, School of Advanced Sciences, VIT-AP University, Amaravati, Andhra Pradesh, India.*

E-mail address: jammula.sp@gmail.com[1]

E-mail address: phanikumarmeduri@gmail.com[2] (corresponding author)